How to cite: *Angew. Chem. Int. Ed.* **2023,** *62,* e202300604
International Edition: doi.org/10.1002/anie.202300604
German Edition: doi.org/10.1002/ange.202300604

Hydrogen Peroxide Production

Contact-electro-catalysis for Direct Synthesis of H_2O_2 under Ambient Conditions

Jiawei Zhao, Xiaotong Zhang, Jiajia Xu, Wei Tang, Zhong Lin Wang,* and Feng Ru Fan**

Abstract: Hydrogen peroxide (H_2O_2) is an indispensable basic reagent in various industries, such as textile bleach, chemical synthesis, and environmental protection. However, it is challenging to prepare H_2O_2 in a green, safe, simple and efficient way under ambient conditions. Here, we found that H_2O_2 could be synthesized using a catalytic pathway only by contact charging a two-phase interface at room temperature and normal pressure. Particularly, under the action of mechanical force, electron transfer occurs during physical contact between polytetrafluoroethylene particles and deionized water/O_2 interfaces, inducing the generation of reactive free radicals ($^{\bullet}OH$ and $^{\bullet}O_2^-$), and the free radicals could react to form H_2O_2, yielding as high as 313 $\mu mol\,L^{-1}\,h^{-1}$. In addition, the new reaction device could show long-term stable H_2O_2 production. This work provides a novel method for the efficient preparation of H_2O_2, which may also stimulate further explorations on contact-electrification-induced chemistry process.

Introduction

Hydrogen peroxide (H_2O_2) is a valuable chemical with great importance in clinical,[1] daily disinfection,[2] organic synthesis,[3] printing industry[4] and other fields. Recently, H_2O_2 also emerges in energy storage as an oxidant and fuel for new fuel cells,[5] avoiding some of the fuel penetration problems. For example, compared with traditional hydrogen fuel cells, it has lower energy price[6] (H_2: 200 $\$\,kW^{-1}$, H_2O_2: 1.84 $\$\,kW^{-1}$). However, H_2O_2 is produced industrially with the well-established anthraquinone oxidation process,[7] which is not an ideal and environmentally friendly method, involving expensive palladium hydrogenation catalysts and generating substantial organic waste from inefficient anthraquinone oxidation. In addition, the logistic issues, including the transportation and storage of unstable and hazardous bulk H_2O_2 solutions, should also be considered. Furthermore, the method of directly generating H_2O_2 from H_2 and O_2 requires precious metals and high-pressure environment, meanwhile, possesses the danger of explosion of H_2 as well,[8] which is not conducive to expanding the scale of production. Hence, an innovative production process of H_2O_2 is desired with green, safety and low-cost under mild reaction conditions.

Using water and oxygen as raw materials to generate H_2O_2 could be an ideal pathway to solve some of these issues. Generally, H_2O_2 production with water and oxygen is an uphill reaction and difficult to perform under ambient conditions, according to the standard Gibbs free energy change[9] (ΔG^0) ($2H_2O + O_2 \rightarrow 2H_2O_2$, $\Delta G^0 = 117\ kJ\,mol^{-1}$). Hence, introducing catalysts into the reactions, for example, photocatalysis[10] and electrocatalysis,[11] could alleviate the problems of slow thermodynamics and kinetics uphill in the reaction process, which are mainly associated with improving the separation/transportation efficiency of electron-hole pairs by tuning the morphology and constructing heterojunction structure. A main challenge to achieve high efficiency for photo/electrocatalytic H_2O_2 production is to enhance the selectivity of the catalytic reaction, that is, to promote the 2e-oxygen reduction reaction (ORR) or the 2e- water oxidation reaction (WOR) while avoiding the 4e- competing reactions.[10a,12] Recently, Zare et al.[13] proposed a micro-droplet method to prepare H_2O_2. They hypothesized that an extremely high electric field formed at the gas-liquid interface of the microdroplet,[14] splitting the hydroxide anion (OH^-) and generating hydroxyl radical ($^{\bullet}OH$) and free electrons. Subsequently, they also found that surface hydroxyl radicals could also be generated during interfacial contact between water and solid, which could recombine and generate H_2O_2.[15] The generation of these hydroxyl radicals may be related to interfacial electron transfer caused by contact electrification at a solid–liquid interface. However, these investigations were carried out at the macroscopic level, and the production yield of H_2O_2 was relatively low.

[*] J. Zhao, X. Zhang, J. Xu, Prof. F. Ru Fan
State Key Laboratory of Physical Chemistry of Solid Surfaces, iChEM, College of Chemistry and Chemical Engineering, Innovation Laboratory for Sciences and Technologies of Energy Materials of Fujian Province (IKKEM), Xiamen University
Xiamen 361005 (China)
E-mail: frfan@xmu.edu.cn
Prof. W. Tang, Prof. Z. Lin Wang
CAS Center for Excellence in Nanoscience, Beijing Institute of Nano energy and Nano systems, Chinese Academy of Sciences
Beijing 100083 (China)
and
School of Nanoscience and Technology, University of Chinese Academy of Sciences
Beijing 100049 (China)
E-mail: tangwei@binn.cas.cn
zhong.wang@mse.gatech.edu
Prof. Z. Lin Wang
Georgia Institute of Technology
Atlanta, GA 30332-0245 (USA)

Our previous study elucidated the mechanism and potential of applying the triboelectric effect to chemical reactions.[16] Recent study showed that the contact-separation cycle between high polymer Fluorinated ethylene propylene (FEP) particles and water under ultrasonication could trigger interfacial electron transfer and induce the generation of reactive oxygen species, realizing efficient degradation of dyes.[17] Therefore, based on contact-electro-catalysis, direct conversion of oxygen and water into H_2O_2 could occur using triboelectrification at the liquid-solid interface under ambient conditions.

In this article, we proposed a facile approach for the direct production of H_2O_2, relying on contact-electro-catalysis between Polytetrafluoroethylene (PTFE) particles and deionized (DI) water without any other traditional catalysts such as noble metals,[18] high-entropy alloys[19] and transition metal oxides.[10b] Under ultrasound treatment, electron exchange could occur between PTFE particles and water with repeated contact and separation cycles at the interface. Electrons could flow from the water to the PTFE surface, resulting in a charged interface that could efficiently catalyze chemical reactions, which usually cannot occur at normal temperature and pressure. We used electron paramagnetic resonance (EPR) to capture intermediate products-free radicals ($^{\bullet}OH$ and $^{\bullet}O_2^-$). Subsequently, we proved that O_2 was involved in the reaction using a $^{18}O_2$ isotope experiment and mass spectrometry (MS). We proposed a contact-electro-catalysis mechanism to generate H_2O_2, where the contact at PTFE-Water and PTFE-O_2 interfaces triggers electron transfer. That could generate free radicals, and the recombination of free radicals produces H_2O_2 (Figure 1a). In addition, the effect of the local high-pressure environment induced by ultrasonication on the reaction was explored by the theoretical simulation method. The results indicated that the high-pressure environment could reduce the energy barrier during the electron transfer process at the two-phase interface, which was more conducive to electron transfer. Next, we confirmed by Raman spectroscopy, scanning electron microscopy (SEM), and X-ray photoelectron spectroscopy (XPS) that the surface structure and chemical composition of the PTFE particles did not change during ultrasonication. This physicochemical stability could be beneficial for the large-scale production of H_2O_2. Thus, we proposed a simple and economical production system based on the principle of contact-electro-catalysis, which achieves long-term stable performance and holds great promise to be applied to more systems, creating a new field of catalysis.

Results and Discussion

The experimental design and reaction pathway for the preparation of H_2O_2 are detailed in Figure 1a. 20 mg of PTFE particles were added into 30 mL of DI water, and the beaker was placed in an ultrasonic bath (40 kHz, 200 W) for sonication. We supposed that a simple system composed of PTFE particles, water and air could produce a large amount of H_2O_2 under normal temperature and pressure. The

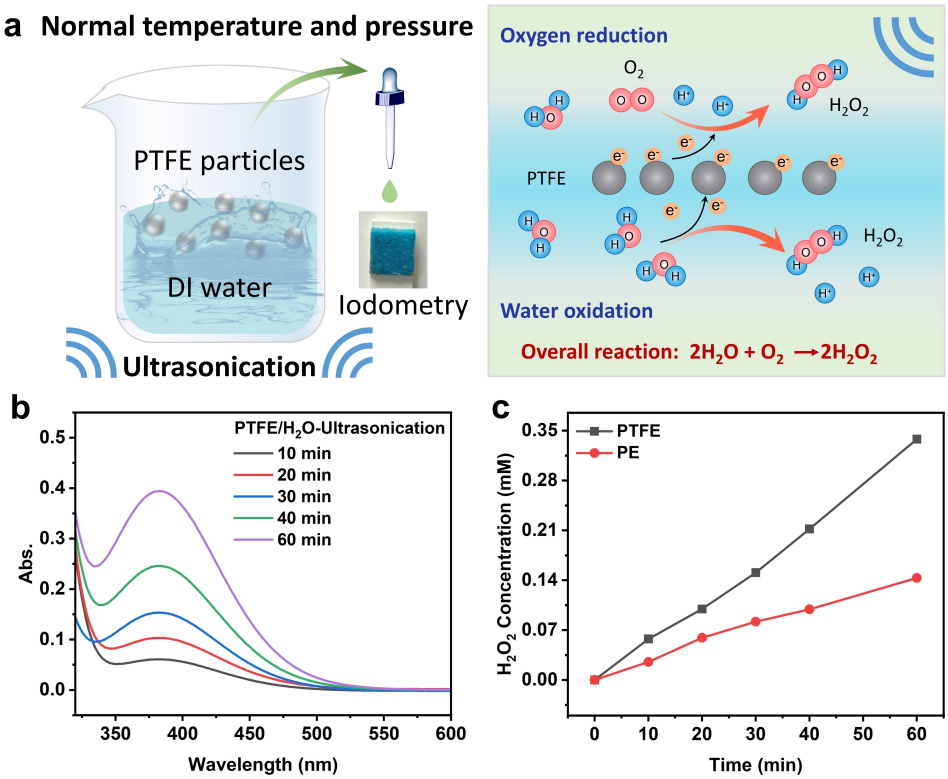

Figure 1. a) Schematic representation of the experimental setup and overall reaction. b) Absorbance variation at different ultrasonic times (using potassium titanium oxalate method). c) Comparison of H_2O_2 yields under PTFE particles and PE particles at different ultrasonic times.

reaction path was based on the fact that PTFE particles could act as electron transfer centers. Simultaneously, water and oxygen could perform oxidation and reduction reactions on the surface of PTFE to realize contact-electro-catalysis and generate H_2O_2. First, we used commercially available H_2O_2 test papers for qualitative testing. The result is shown in Figure 1a, where the test paper turned blue,[20] indicating the presence of H_2O_2. Then, we used the method based on the potassium titanium oxalate[15,21] and potassium permanganate[22] to quantify the concentration of H_2O_2. Herein, H_2O_2 could undergo a coordination reaction with Ti^{4+} in potassium titanium oxalate to form a stable yellow complex, which has a characteristic absorbance peak at 385 nm, linearly related to the concentration of H_2O_2. In addition, H_2O_2 and potassium permanganate undergo a redox reaction in an acidic environment, and the original purple color of the potassium permanganate solution is reduced to colorless. The absorbance of the characteristic absorption peak (525 nm) decreases as the concentration of H_2O_2 increases (Figure S1a–b). The concentration of H_2O_2 after 40 min of ultrasonication was calculated by the standard curve of the potassium permanganate and potassium titanium oxalate method (Figure S2a–b), which were 170.0 μmol L^{-1} and 195.8 μmol L^{-1}, respectively.

The concentrations of H_2O_2 under different ultrasonication times (10, 20, 30, 40 and 60 min) were tested by UV-Vis spectroscopy. Focusing on the method based on potassium titanium oxalate, it was found that the standard absorption peak intensity increased continuously with the ultrasonication time (Figure 1b), indicating that the concentration of H_2O_2 has a linear relationship with the increase in reaction time. Furthermore, we performed a series of control experiments under different conditions. In the absence of PTFE particles, or mechanical stirring (800 rpm) was used instead of ultrasonic treatment, the results of two control experiments showed no H_2O_2 generation (Figure S3), proving the existence of PTFE particles and ultrasonic treatment are necessary to obtain H_2O_2.

Previous studies have shown that polymers with high dielectric constant could strongly attract negative charges.[23] After the PTFE film is contacted and separated from water, a large amount of negative charge will accumulate on the surface of the PTFE. To verify the universality of the catalytic synthesis of H_2O_2 driven by the contact electrification between polymer and water, we used other Polyethylene (PE) particles with a slightly lower dielectric constant than PTFE.[23c,24] The results indicated that the interaction between PE particles and water could also directly catalyze the synthesis of H_2O_2. However, its yield was about 40 % lower than that of PTFE under the same conditions (Figure 1c). This showed that the yield of H_2O_2 is directly related to the polymer's position in the triboelectric series and its ability to attract electrons after contact electrification with water. We also selected other materials with different physical properties, including fluorinated ethylene propylene (FEP), AlN, polyvinylidene fluoride (PVDF), polydimethylsiloxane (PDMS) nanoparticles and ethyl cellulose, and carried out quantitative tests on the generated H_2O_2. as shown in Figure S4a–b. Our experimental findings indicate that this method has wide applicability and strong universality due to the diverse range of materials available for selection. Our study underlined that the catalytic performance is related to the nature of the applied materials. The relationship between the performance of contact-electro-catalysis (including reaction rate and selectivity) and materials in different systems remains to be further studied and explored.

Triboelectric charging can harvest mechanical energy, such as typical triboelectric nanogenerators, and drive chemical reactions. Grzybowski et al. found that radicals created by solid-solid triboelectrification rather than transferred electrons are responsible for promoting electrochemical reduction.[25] To reveal the underlying mechanism of solid–liquid triboelectrically driven synthesis of H_2O_2, we first investigated whether the strong ultrasonication will change the physical and chemical properties of the PTFE particles' surface. We performed morphological characterization and element mapping analysis of PTFE particles before and after the reaction by scanning electron microscopy with energy dispersive X-ray analysis (SEM-EDX). Figure S5a–b illustrates that the morphology and element distribution of PTFE particles did not change during/after the catalytic process. X-ray diffractometry (XRD) analysis,[26] Raman spectroscopy,[27] and Fourier transform infrared (FTIR) spectroscopy[28] were used to explore whether the chemical properties of PTFE particles changed (Figure 2a–c). The results indicated that the structure and properties of PTFE particles did not change after the ultrasonication process.

Next, the chemical state of PTFE particles before and after the reaction was analyzed by XPS.[17,28] The spectral information of C1s, F1s and O1s are shown in Figure 2d. The original peak did not change, and no newly formed peaks were observed on the surface of PTFE. To explore whether the PTFE particles decompose under the action of external mechanical force, we separated the solid and liquid of the reaction solution and performed FTIR and Raman tests on the filtered aqueous solutions. The characteristic peaks of polymer materials did not appear (Figure S6a–b), confirming that the chemical properties of PTFE particles remained stable. Considering these results, we considered that the generation of H_2O_2 was mainly based on the contact-electro-catalysis between PTFE particles and DI water under ultrasonication rather than the catalysis of mechanical free radicals or other molecular charged fragments generated by the breakage of polymer surface molecules.

To reveal the formation mechanism for H_2O_2, the characterization of the intermediates during the contact-electro-catalytic reaction was investigated systematically. We used electron paramagnetic resonance (EPR) spectroscopy[29] and electron sacrificial agents to identify intermediate products, confirming the pathways of charge transfer and H_2O_2 generation. Three test methods were designed:[30] a 100 mM DMPO solution, a solution containing both 100 mM DMPO and 1 mM DMSO, and a 100 mM TEMP solution. DMSO was used to quench $^{\bullet}OH$ radicals, increasing the opportunities for DMPO to capture superoxide radicals. As shown in Figure 3a–c, after the introduction of ultrasonication, the first group of measurements produced quadruplet DMPO-$^{\bullet}OH$ characteristic peaks (Figure 3a), which are generated by OH^-

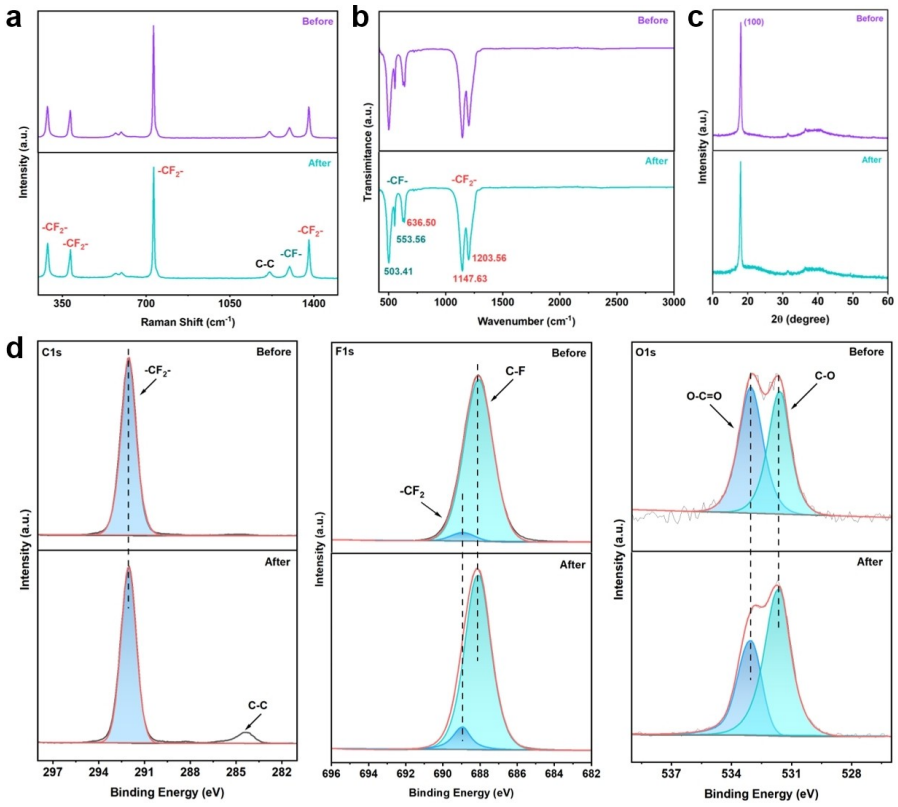

Figure 2. a) Raman spectra, (b) FTIR spectra and (c) XRD pattern of PTFE particles before and after the reaction. d) C1s, F1s, and O1s XPS spectra of PTFE particles before and after the reaction.

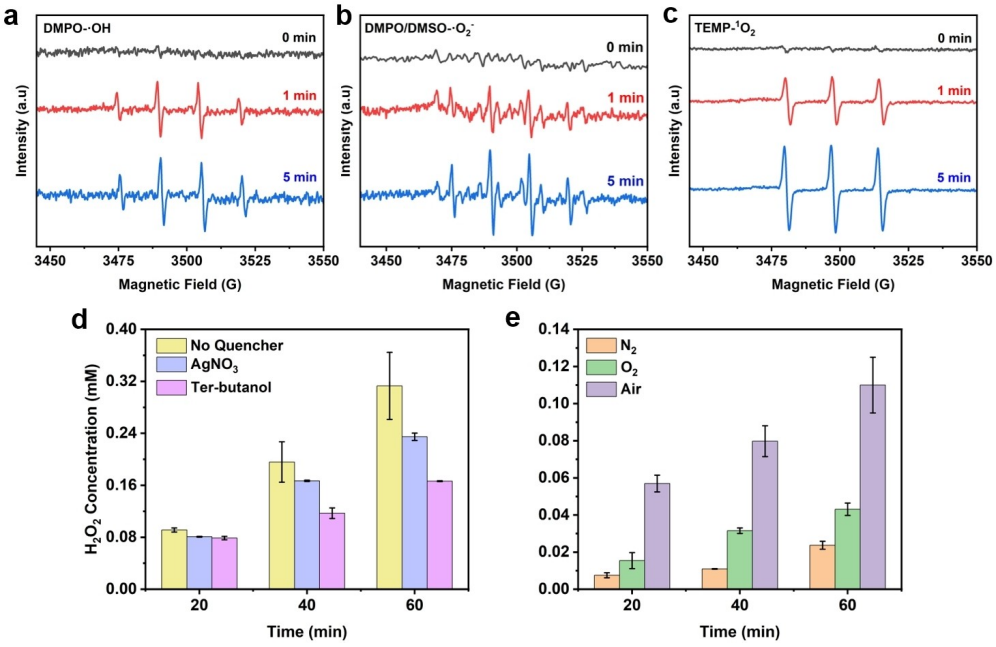

Figure 3. EPR spectra for (a) DMPO-•OH, (b) DMPO/DMSO-•O_2^-, (c) TEMP-$^1O_2$ in the presence of PTFE particles during ultrasonication in air atmosphere. d) Evolution of H_2O_2 in the presence of various radical scavengers. e) Investigation of the effect of dissolved gases on H_2O_2 production.

or (H_2O) in solution by electron-transfer-type oxidation reactions.[31] In comparison, the second group of tests produced sextuplet weaker characteristic peaks of DMPO-•O_2^- (Figure 3b), generated by O_2 gaining electrons. The

entire profile was dominated by a quadruplet DMPO-•OH peak, ascribed to the fact that hydroxyl radicals are more prone to react with DMPO. Moreover, the third group of tests showed stronger triplet TEMP-$^1O_2$ characteristic peaks (Figure 3c) as the oxidation product of $•O_2^-$. These results showed that PTFE particles and water could generate the three kinds of free radicals during ultrasonication, and the generation amount increases with ultrasonication time.

Next, we added $AgNO_3$ (1 mM) as the electron sacrificial agent and the free radical quencher tert-butanol (1 mM) to the reaction to examine whether the radicals were produced by electron transfer.[17] Control experiments were performed to exclude interfering factors produced by the sacrificial agent on the standard peak absorbance (Figure S7). The results in Figure 3d showed that the production of H_2O_2 could be reduced by introducing either an electron sacrificial agent or a radical quencher. The H_2O_2 concentrations obtained in the presence of the electron sacrificial agent group and free radical quencher group were 0.231 mmol L^{-1} and 0.166 mmol L^{-1}, respectively, which proved that introducing a sacrificial agent could affect the electron transfer during the electrification of interface contact.

In this system, in addition to the PTFE particles, O_2 was also involved in the reaction, playing an essential role. To explore the relationship between the amount of dissolved oxygen in the water and the yield of as-produced H_2O_2, we applied different atmospheres (Air/O_2/N_2) into the reaction chamber. The results in Figure 3e showed that the concentration of H_2O_2 in the air atmosphere was the highest, up to 0.106 mmol L^{-1}, followed by the pure oxygen atmosphere with a concentration of 0.043 mmol L^{-1}, while the concentration of H_2O_2 in the N_2 atmosphere was only 0.024 mmol L^{-1}. The results showed that oxygen is one of the main reactants to generate H_2O_2, following our results of trapping oxygen-based radicals. Compared with the air atmosphere, the lower production of H_2O_2 in pure oxygen could be attributed to the oxidative properties of oxygen, reducing the contact electrification performance between materials,[32] thereby lowering the total amount of transferred charges and the generation of free radicals.

The concentration of ions in the water could also affect the production of H_2O_2.[33] If the ion concentration is too high, an ion shielding effect could occur at the interface, inhibiting electron transfer. To investigate this aspect, we added large amounts of NaCl to DI water and found that the production of H_2O_2 was significantly reduced with the addition of salt (Figure S8). The results showed that electron transfer occurred during the interface contact electrification process. Since the electrons are transferred to different substrates, different free radicals are induced, and the free radicals could combine to generate H_2O_2. In general, the conditions unfavorable (such as humidity and atmosphere) for contact electrification will directly reduce the yield of H_2O_2.[16]

Based on the above characterization results, we have examined the pathway for the generation of H_2O_2 catalyzed by contact electrification, divided into two half-reactions, water oxidation and oxygen reduction (Figure 4a). For the water oxidation, after the PTFE particles are contacted and separated from water, the electrons of water are transferred to the surface of PTFE particles, forming water radical cations. These cations then form hydronium cations and hydroxyl radicals, which combine to form H_2O_2.[34] This pathway is a one-electron process of the water oxidation reaction (WOR).[35] However, due to the high thermodynamic potential required to generate •OH, it is difficult to find proper catalysts that are still stable under such extreme anodic bias. To the authors' best knowledge, no electrocatalysts have been demonstrated to exhibit proper energetics for direct ·OH generation.[36] Therefore, the production of H_2O_2 via this route could present great advantages.

For the oxygen reduction pathway, oxygen dissolved in water continuously generates a large number of small bubbles under ultrasound treatment. These bubbles will continue to expand and then collapse and disappear. During this process, multiple solid–gas and liquid–gas interfaces are formed. Oxygen in the bubbles obtains electrons from the surface of PTFE particles to form $•O_2^-$. These radicals could combine with H^+ in the aqueous solution to form •OOH, which will gain electrons again and combine with H^+ to form H_2O_2. Meanwhile, the PTFE particles that lost electrons will return to their original state again. This pathway is called the oxygen reduction reaction (ORR),[12b] and its mechanism is similar to the photocatalytic 2e$^-$-ORR process.[10a,37] Herein, the reduction of O_2 to $•O_2^-$ is a rate-limiting step, requiring a more negative potential (−0.33 V) to proceed than the 2e$^-$-ORR (+0.68 V) process. Hence, the $•O_2^-$ could be further oxidized to form a single $^1O_2$ as a side reaction (Figure 3c).

We also confirmed that O_2 was involved in the generation of H_2O_2 by the $^{18}O_2$ isotope experiment and liquid chromatography coupled with mass spectrometry (LC-MS)[15] (Figure S9). The results of LC-MS also showed that the yield of H_2O_2 produced by the WOR pathway was higher than that of the 2e$^-$-ORR pathway. Therefore, a part of the O_2 may generate H_2O through 4e$^-$-ORR pathway. In general, ultrasonication caused frequent contact-separation cycles between PTFE particles and water, while electrons completed cyclic transfer at different solid–liquid–gas interfaces on the surface of PTFE. As long as the external mechanical force was applied, the cyclic reaction continued to generate H_2O_2.

When the high-energy ultrasonic wave acts on the liquid, it produces a cavitation effect,[30,38] generating local high-pressure and high heat. Considering the influence of the ultrasonic environment on interfacial electron transfer, the energy barriers for realizing these electron exchange processes were calculated by Density Functional Theory (DFT). The high-pressure environment generated by bubble collapse was simulated, and the details are available in Supporting Information. In the two cases of H_2O/PTFE and PTFE*/O_2 (Figure S10), the energy band gap between LUMO and HOMO gradually decreased as the system's volume was compressed. When the volume was compressed to 64.0 % of the original volume (Figure 4b), the calculation results showed that the energy barriers for electron transfer were reduced by 16.9 % and 16.3 %, respectively. Therefore, high-frequency interfacial contact could increase the chances of electron transfer, and the local high-pressure environment could decrease the energy barriers to facilitate electron transfer.

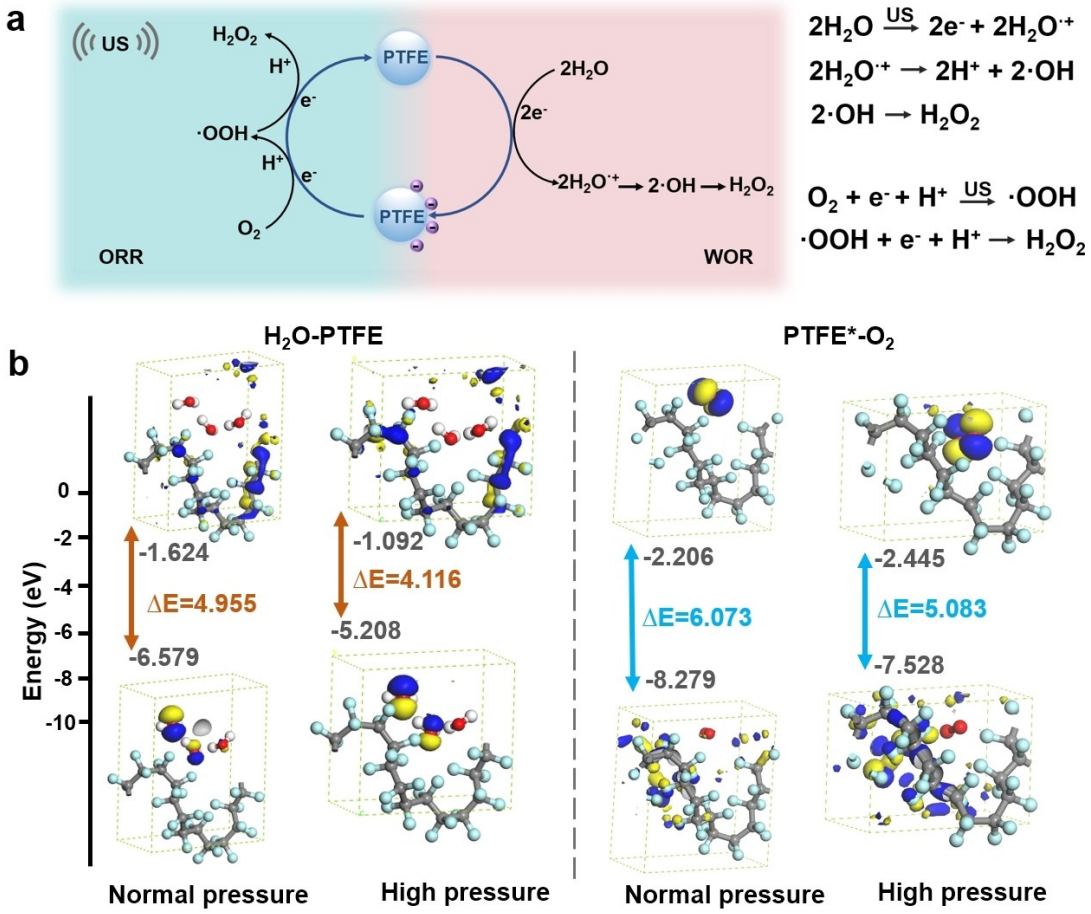

Figure 4. a) Proposed reaction mechanism of contact-electro-catalysis for H_2O_2 generation. b) DFT calculations of the values of LUMO and HOMO levels for H_2O-PTFE and O_2-PTFE in various conditions.

Previous experimental results showed that the yield of H_2O_2 could be directly related to the amount of transferred charges on the surface. Subsequently, to explore other factors that may affect the yield of H_2O_2 and to improve the catalytic efficiency, we carried out a series of comparative experiments encompassing different amounts and sizes of PTFE particles, different powers and frequencies of ultrasonic cleaner. First, 20 mg of PTFE particles with different particle sizes were added to the same volume (30 mL) of DI water with ultrasonic treatment for 40 minutes (Figure 5a). PTFE particles with sizes of 1.6 μm and 3.0 μm had the highest yields of H_2O_2, 0.297 mmol L^{-1} h^{-1} and 0.294 mmol L^{-1} h^{-1}, respectively. The H_2O_2 yields of the smallest particle size group of 0.2 μm and the largest particle size group of 25 μm were the lowest, 0.221 mmol L^{-1} h^{-1} and 0.215 mmol L^{-1} h^{-1}, respectively. PTFE particles with smaller particle sizes have a larger specific surface area and tend to transfer more electrons.[33] However, the particles with too small particle sizes do not benefit from gaining more electrons on the surface, indicating that PTFE particles with larger or smaller particle sizes are not favorable to electron transfer and aggregation.

Next, the variation law of H_2O_2 concentration of PTFE particles with a particle size of 3 μm with different quantities was explored. As shown in Figure 5b, 10, 20, 30, and 40 mg of PTFE particles were added to 30 mL of DI water, respectively. The concentration of H_2O_2 increased first and then decreased with the increase of the applied PTFE quantity. The yield of 40 mg PTFE particles was 0.233 mmol L^{-1} h^{-1}, 17.5 % lower than the 10 mg. This reveals that more PTFE particles increase the contact chance of the solid/liquid interface, contributing to an efficient electron transfer. However, the accumulation of electrons at the interface could form a high electric field, which is not conducive to the re-transfer of more electrons, inhibiting the generation of free radicals and reducing the yield of H_2O_2.

In addition, the frequency and power of ultrasonic treatment could also affect the yield of H_2O_2.[39] We have chosen four different powers of 40, 60, 80, and 100 W for comparative experiments (Figure 5c). The yield of H_2O_2 increased with the increment of the power, but the magnitude of the increase decreased. When the power was 100 W, and the frequency was 500 kHz, the H_2O_2 concentration was only 0.0057 mmol L^{-1} after high-frequency ultrasonic treatment for 40 min (Figure S11). A high ultrasonic frequency means a fast oscillation frequency, which could enhance the contact separation of the interface.[40] However, if the oscillation frequency was too high, the wavelength became shorter. In this way, the attenuation in the propagation process increases,

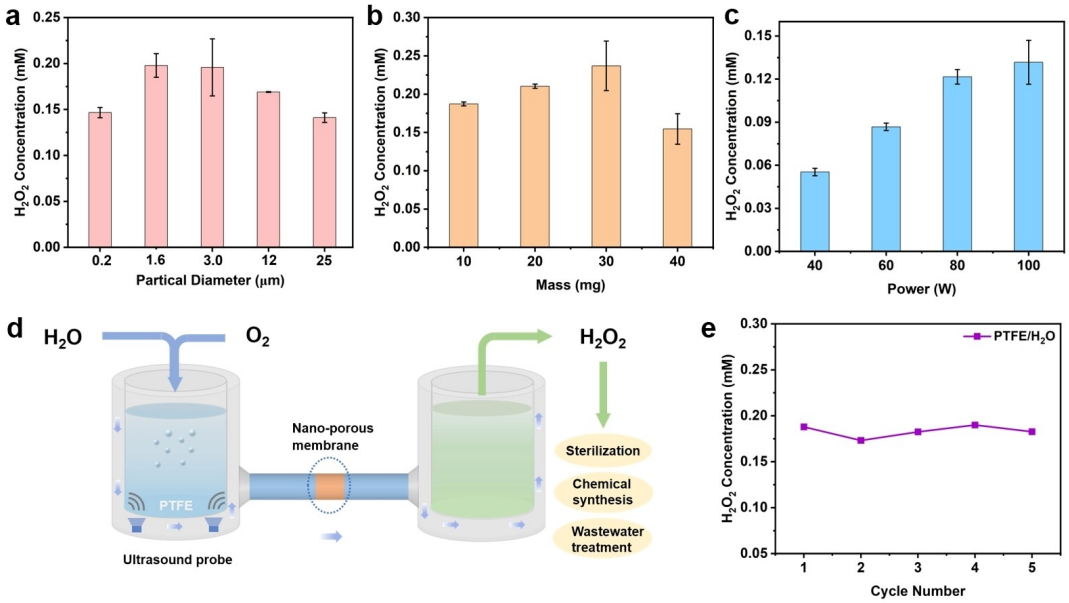

Figure 5. Comparison of H_2O_2 yields under (a) different particle diameters and (b) different amounts of PTFE particles. c) Concentrations of H_2O_2 under different applied powers of ultrasonic cleaner. d) Expected large application of contact-electro-catalysis technology in the field of efficient production of H_2O_2. e) Cycling performance for H_2O_2 production.

and the utilization rate of ultrasonic energy decreases. These experiments showed that the energy value of ultrasonic input positively correlates with the yield of H_2O_2.

Contact electrification is a common phenomenon in daily life, and polymer materials are cheap and easy to obtain.[24] Therefore, we designed an economic H_2O_2 production system based on the principle of contact-electro-catalysis. The design idea (Figure 5d) is expected to be mass-produced and accelerate the commercialization of contact electrocatalysis production of H_2O_2. To prove the system's feasibility, we built a simple experimental device (Figure S12) and verified the method's stability. As shown in Figure 5e, the H_2O_2 yield of the device can still reach the initial 97.2 % after 5 cycles, indicating its high durability. It could also be seen that the preparation of H_2O_2 by using contact electrification can simplify the preparation steps, reduce the economic cost and realize the whole green production.

Conclusion

We have explored a new approach for chemical synthesis of H_2O_2 at ambient condition without using any conventional catalysis. The results showed that 195.8 μmol L^{-1} of H_2O_2 was successfully obtained by adding 20 mg of PTFE particles to 30 mL of DI water with 40 min ultrasonication. The specific reaction pathways have been investigated experimentally, employing the electron-catalyzed chemical reaction transferred during the contact electrification process of the two substances to build an electron cycle transfer system between DI water and PTFE particles, PTFE particles and oxygen. The transfer of electrons initiates the production of free radicals, which are further combined to form H_2O_2. In addition, by comparing the yields of H_2O_2 under different experimental conditions, the general rules affecting the electrocatalytic efficiency of contact-electro-catalysis can be summarized. This could be improved by appropriately reducing the polymer particle size to about 1–10 μm, increasing the contact area and ultrasonic power, or introducing chemical modifications to the surface. Increasing the amounts of as-transferred electrons could further improve the catalytic efficiency. This contact-electro-catalysis method is a brand-new catalytic pathway with wider material selection and stronger electrification advantages. Finally, according to our results, it is of great scientific significance to expand the application field of contact-electro-catalysis.

Acknowledgements

This work was supported by the National Natural Science Foundation of China (22222305 and 22021001), the Fundamental Research Funds for the Central Universities (20720220013). We especially thank Jiahan Song, Gan Liu, Xianmeng Song, Yanjie Wang, Jianing Dong, Siying Huang, Weishen Song, Ziang Nan and Xi Jin for helpful discussions.

Conflict of Interest

The authors declare no conflict of interest.

Data Availability Statement

The data that support the findings of this study are available in the Supporting Information of this article.

Keywords: Contact Electrification · Electrocatalysis · Hydrogen Peroxide · Polytetrafluoroethylene · Ultrasonication

[1] R. Hage, A. Lienke, *Angew. Chem. Int. Ed.* **2005**, *45*, 206–222.
[2] R. Ciriminna, L. Albanese, F. Meneguzzo, M. Pagliaro, *ChemSusChem* **2016**, *9*, 3374–3381.
[3] a) N. Agarwal, S. J. Freakley, R. U. McVicker, S. M. Althahban, N. Dimitratos, Q. He, D. J. Morgan, R. L. Jenkins, D. J. Willock, S. H. Taylor, C. J. Kiely, G. J. Hutchings, *Science* **2017**, *358*, 223–227; b) B. Puértolas, A. K. Hill, T. García, B. Solsona, L. Torrente-Murciano, *Catal. Today* **2015**, *248*, 115–127.
[4] Y. Wu, J. Wu, F. Yang, C. Tang, Q. Huang, *Polymer* **2019**, *11*, 776.
[5] a) K. Mase, M. Yoneda, Y. Yamada, S. Fukuzumi, *Nat. Commun.* **2016**, *7*, 11470; b) S. Fukuzumi, *Joule* **2017**, *1*, 689–738.
[6] A. Aytaç, M. Gürbüz, A. E. Sanli, *Int. J. Hydrogen Energy* **2011**, *36*, 10013–10021.
[7] J. M. Campos-Martin, G. Blanco-Brieva, J. L. Fierro, *Angew. Chem. Int. Ed.* **2006**, *45*, 6962–6984.
[8] a) S. Chinta, *J. Catal.* **2004**, *225*, 249–255; b) S. J. Freakley, Q. He, J. H. Harrhy, L. Lu, D. A. Crole, D. J. Morgan, E. N. Ntainjua, J. K. Edwards, A. F. Carley, A. Y. Borisevich, C. J. Kiely, G. J. Hutchings, *Science* **2016**, *351*, 965–968; c) J. K. Edwards, S. J. Freakley, R. J. Lewis, J. C. Pritchard, G. J. Hutchings, *Catal. Today* **2015**, *248*, 3–9.
[9] W. Fan, B. Zhang, X. Wang, W. Ma, D. Li, Z. Wang, M. Dupuis, J. Shi, S. Liao, C. Li, *Energy Environ. Sci.* **2020**, *13*, 238–245.
[10] a) H. Hou, X. Zeng, X. Zhang, *Angew. Chem. Int. Ed.* **2020**, *59*, 17356–17376; b) L. Wang, J. Zhang, Y. Zhang, H. Yu, Y. Qu, J. Yu, *Small* **2022**, *18*, 2104561; c) Y. Ding, S. Maitra, S. Halder, C. Wang, R. Zheng, T. Barakat, S. Roy, L.-H. Chen, B.-L. Su, *Matter* **2022**, *5*, 2119–2167.
[11] a) X. Hu, Z. Sun, G. Mei, X. Zhao, B. Y. Xia, B. You, *Adv. Energy Mater.* **2022**, *12*, 2201466; b) L. Fan, X. Bai, C. Xia, X. Zhang, X. Zhao, Y. Xia, Z. Y. Wu, Y. Lu, Y. Liu, H. Wang, *Nat. Commun.* **2022**, *13*, 2668.
[12] a) X. Shi, S. Siahrostami, G.-L. Li, Y. Zhang, P. Chakthranont, F. Studt, T. F. Jaramillo, X. Zheng, J. K. Nørskov, *Nat. Commun.* **2017**, *8*, 701; b) N. Wang, S. Ma, P. Zuo, J. Duan, B. Hou, *Adv. Sci.* **2021**, *8*, 2100076.
[13] a) J. K. Lee, H. S. Han, S. Chaikasetsin, D. P. Marron, R. M. Waymouth, F. B. Prinz, R. N. Zare, *Proc. Natl. Acad. Sci. USA* **2020**, *117*, 30934–30941; b) M. A. Mehrgardi, M. Mofidfar, R. N. Zare, *J. Am. Chem. Soc.* **2022**, *144*, 7606–7609.
[14] a) C. Gong, D. Li, X. Li, D. Zhang, D. Xing, L. Zhao, X. Yuan, X. Zhang, *J. Am. Chem. Soc.* **2022**, *144*, 3510–3516; b) J. K. Lee, D. Samanta, H. G. Nam, R. N. Zare, *J. Am. Chem. Soc.* **2019**, *141*, 10585–10589.
[15] B. Chen, Y. Xia, R. He, H. Sang, W. Zhang, J. Li, L. Chen, P. Wang, S. Guo, Y. Yin, L. Hu, M. Song, Y. Liang, Y. Wang, G. Jiang, R. N. Zare, *Proc. Natl. Acad. Sci. USA* **2022**, *119*, e2209056119.
[16] F.-R. Fan, S. Xie, G.-W. Wang, Z.-Q. Tian, *Sci. China Chem.* **2021**, *64*, 1609–1613.
[17] Z. Wang, A. Berbille, Y. Feng, S. Li, L. Zhu, W. Tang, Z. L. Wang, *Nat. Commun.* **2022**, *13*, 130.
[18] Z. Teng, Q. Zhang, H. Yang, K. Kato, W. Yang, Y.-R. Lu, S. Liu, C. Wang, A. Yamakata, C. Su, B. Liu, T. Ohno, *Nat. Catal.* **2021**, *4*, 374–384.
[19] a) J. K. Edwards, S. J. Freakley, A. F. Carley, C. J. Kiely, G. J. Hutchings, *Acc. Chem. Res.* **2014**, *47*, 845–854; b) J. K. Edwards, B. Solsona, E. Ntainjua, N. A. F. Carley, A. A. Herzing, C. J. Kiely, G. J. Hutchings, *Science* **2009**, *323*, 1037–1041.
[20] T. M. Gill, X. Zheng, *Chem. Mater.* **2020**, *32*, 6285–6294.
[21] N. H. Musskopf, A. Gallo, Jr., P. Zhang, J. Petry, H. Mishra, *J. Phys. Chem. Lett.* **2021**, *12*, 11422–11429.
[22] A. Izgorodin, E. Izgorodina, D. R. MacFarlane, *Energy Environ. Sci.* **2012**, *5*, 9496.
[23] a) F.-R. Fan, Z.-Q. Tian, Z. Lin Wang, *Nano Energy* **2012**, *1*, 328–334; b) H. Zou, Y. Zhang, L. Guo, P. Wang, X. He, G. Dai, H. Zheng, C. Chen, A. C. Wang, C. Xu, Z. L. Wang, *Nat. Commun.* **2019**, *10*, 1427; c) Z. L. Wang, A. C. Wang, *Mater. Today* **2019**, *30*, 34–51.
[24] D. J. Lacks, T. Shinbrot, *Nat. Chem. Rev.* **2019**, *3*, 465–476.
[25] B. Baytekin, H. T. Baytekin, B. A. Grzybowski, *J. Am. Chem. Soc.* **2012**, *134*, 7223–7226.
[26] L. Zheng, J. Zhou, J. Shen, W. Chen, Y. Qi, S. Shen, S. Li, *J. Mater. Sci. Mater. Electron.* **2017**, *28*, 11665–11670.
[27] E. Wyszkowska, M. Leśniak, L. Kurpaska, R. Prokopowicz, I. Jozwik, M. Sitarz, J. Jagielski, *J. Mol. Struct.* **2018**, *1157*, 306–311.
[28] J. Piwowarczyk, R. Jedrzejewski, D. Moszynski, K. Kwiatkowski, A. Niemczyk, J. Baranowska, *Polymer* **2019**, *11*, 1629.
[29] R. Li, Y. Weng, X. Zhou, X. Wang, Y. Mi, R. Chong, H. Han, C. Li, *Energy Environ. Sci.* **2015**, *8*, 2377–2382.
[30] Y. Wang, Y. Xu, S. Dong, P. Wang, W. Chen, Z. Lu, D. Ye, B. Pan, D. Wu, C. D. Vecitis, G. Gao, *Nat. Commun.* **2021**, *12*, 3508.
[31] R. Nakamura, T. Okamura, N. Ohashi, A. Imanishi, Y. Nakato, *J. Am. Chem. Soc.* **2005**, *127*, 12975–12983.
[32] L. L. Sun, S. Q. Lin, W. Tang, X. Chen, Z. L. Wang, *ACS Nano* **2020**, *14*, 17354–17364.
[33] J. Nie, Z. Ren, L. Xu, S. Lin, F. Zhan, X. Chen, Z. L. Wang, *Adv. Mater.* **2020**, *32*, 1905696.
[34] M. T. Dulay, C. A. Huerta-Aguilar, C. F. Chamberlayne, R. N. Zare, A. Davidse, S. Vukovic, *QRB Discovery* **2021**, *2*, e8.
[35] S. Siahrostami, S. J. Villegas, A. H. Bagherzadeh Mostaghimi, S. Back, A. B. Farimani, H. Wang, K. A. Persson, J. Montoya, *ACS Catal.* **2020**, *10*, 7495–7511.
[36] a) X. Shi, S. Back, T. M. Gill, S. Siahrostami, X. Zheng, *Chem* **2021**, *7*, 38–63; b) P.-A. Michaud, M. Panizza, L. Ouattara, T. Diaco, G. Foti, C. Comninellis, *J. Appl. Electrochem.* **2003**, *33*, 151–154; c) S. Mavrikis, M. Göltz, S. Rosiwal, L. Wang, C. Ponce de León, *ChemSusChem* **2022**, *15*, e202102137.
[37] Y. Nosaka, A. Y. Nosaka, *Chem. Rev.* **2017**, *117*, 11302–11336.
[38] P. Tao, C. Yang, H. Wang, Y. Zhao, X. Zhang, M. Shao, T. Sun, *J. Environ. Chem. Eng.* **2021**, *9*, 104905.
[39] P. Vasandani, Z.-H. Mao, W. Jia, M. Sun, *J. Electrost.* **2017**, *90*, 147–152.
[40] I. Gültekin, G. Tezcanli-Guyer, N. H. Ince, *Ultrason. Sonochem.* **2009**, *16*, 577–581.

Manuscript received: January 12, 2023
Accepted manuscript online: March 22, 2023
Version of record online: April 17, 2023